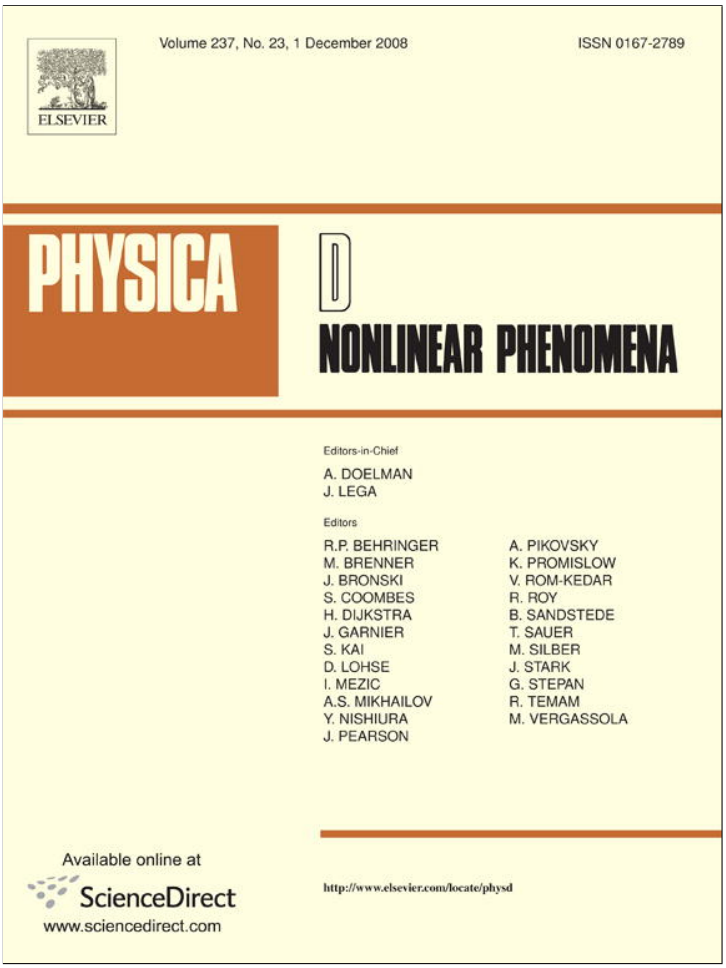

Physica D 237 (2008) 3061–3068

Contents lists available at ScienceDirect

Physica D

journal homepage: www.elsevier.com/locate/physd

Switching to nonhyperbolic cycles from codim 2 bifurcations of equilibria in ODEs

Yu.A. Kuznetsov [a], H.G.E. Meijer [b,*], W. Govaerts [c], B. Sautois [c]

[a] Department of Mathematics, Utrecht University, Budapestlaan 6, 3584CD Utrecht, The Netherlands

[b] Department of Applied Mathematics, Twente University, P.O. Box 217, 7500 AE, Enschede, The Netherlands

[c] Department of Applied Mathematics and Computer Science, Ghent University, Krijgslaan 281-S9, B-9000 Ghent, Belgium

ARTICLE INFO

Article history:
Received 21 January 2008
Received in revised form
13 June 2008
Accepted 18 June 2008
Available online 27 June 2008
Communicated by B. Sandstede

Keywords:
Codimension-two bifurcation
Normal form
Branch switching
Periodic orbits

ABSTRACT

The paper provides full algorithmic details on switching to the continuation of all possible codim 1 cycle bifurcations from generic codim 2 equilibrium bifurcation points in n-dimensional ODEs. We discuss the implementation and the performance of the algorithm in several examples, including an extended Lorenz-84 model and a laser system.

1. Introduction

Consider a system of differential equations depending on two parameters

$$\dot{x} = f(x, \alpha), \quad (x, \alpha) \in \mathbb{R}^n \times \mathbb{R}^2, \tag{1}$$

where f is smooth. In general, there are bifurcation curves in the α-plane, at which the system exhibits codim 1 bifurcations, for example, fold or Hopf bifurcations of equilibrium points. Moreover, generically, one expects points of codim 2 bifurcations, where several curves corresponding to codim 1 bifurcations intersect transversally or tangentially. A codim 2 point is of particular interest if it is not only the origin of some equilibrium bifurcation curves but also of some curves corresponding to bifurcations of periodic orbits (cycles). Such points can be detected by purely local analysis of equilibria and then be used to establish the existence of limit cycle bifurcations and other global phenomena that could hardly be proved otherwise. That is why codim 2 points are often called the "organizing centers" in applied literature.

The theory of codim 2 bifurcations of equilibria in generic systems (1) is well developed (see, for example, [1,11,17]). There are five well-known codim 2 equilibrium bifurcations: cusp (CP), Bautin (generalized Hopf, GH), double zero (Bogdanov-Takens, BT), zero-Hopf (ZH), and double Hopf (HH). It follows from their analysis that branches of nonhyperbolic limit cycles can emanate from GH, ZH and HH points only. More precisely, a codim 1 bifurcation curve LPC, along which a cycle with a nontrivial multiplier $\mu_1 = 1$ exists, emanates from a generic GH point, while codim 1 bifurcation curves NS, along which a cycle with a pair of multipliers $\mu_{1,2} = e^{\pm i\theta}$ exists, are rooted at generic ZH and HH points. Notice that NS is used to denote both Neimark–Sacker and neutral saddle cycles where $\mu_1\mu_2 = 1$ and that no period-doubling curves can emanate from generic codim 2 equilibrium bifurcations.

Obviously, the application of these theoretical results to realistic models (1) is impossible without numerical tools. The numerical analysis of a codim 2 equilibrium bifurcation includes:

- detection and location of the point along a branch of a codim 1 bifurcation;
- computation of the coefficients of the normal form of the restriction of (1) to the critical center manifold at the bifurcation parameter values and checking the nondegeneracy conditions;
- verification of the transversality of the given family (1) to the codim 2 bifurcation manifold and establishing a correspondence between the unfolding parameters of the normal form and original system parameters α;
- computing accurate approximations of the codim 1 curves in the α-space and the corresponding singular orbits in the x-space near the bifurcation, sufficient to initialize the

* Corresponding author. Tel.: +31 534893416.
E-mail address: meijerhge@math.utwente.nl (H.G.E. Meijer).

0167-2789/$ – see front matter © 2008 Elsevier B.V. All rights reserved.
doi:10.1016/j.physd.2008.06.006

numerical continuation of these codim 1 curves using only local information available at the codim 2 point.

While the first two problems were studied in detail (see [3] and references therein) and have been implemented into the standard bifurcation software CONTENT [19] and MATCONT [6], the two last issues received much less attention in the numerical analysis literature in the case of bifurcations of nonhyperbolic cycles. The present paper is aimed at bridging this gap by providing full algorithmic details on switching to all possible codim 1 cycle bifurcations from generic GH, ZH and HH codim 2 points.

One way to set up a computational switching procedure is to consider a smooth normal form for the codim 2 bifurcation including the parameters $\beta \in \mathbb{R}^2$

$$\dot{w} = G(w, \beta), \qquad G : \mathbb{R}^{n_c} \times \mathbb{R}^2 \to \mathbb{R}^{n_c}. \tag{2}$$

For all codim 2 equilibrium bifurcations these normal forms are known. Suppose that an exact or approximate formula is available that gives the emanating codim 1 bifurcations for the normal form (2). In order to transfer this to the original equation (1) we need a relation

$$\alpha = V(\beta), \qquad V : \mathbb{R}^2 \to \mathbb{R}^2, \tag{3}$$

between the unfolding parameters β and the given parameters α. In our context, V will be linearly approximated. Moreover, we need a center manifold parametrization

$$x = H(w, \beta), \qquad H : \mathbb{R}^{n_c} \times \mathbb{R}^2 \to \mathbb{R}^n, \tag{4}$$

that incorporates β. Taking (3) and (4) together, the invariance condition for the parameter-dependent center manifold in the ODE (1) can be written as a *homological equation*:

$$H_w(w, \beta)G(w, \beta) = f(H(w, \beta), V(\beta)), \tag{5}$$

which we can solve by a recursive procedure based on Fredholm's solvability condition that will give the Taylor coefficients of G, H with respect to w and β and V w.r.t. to β. We assume that G is normalized, i.e. the zero coefficients in the Taylor series of G are known in the expansion

$$G(w, \beta) = \sum_{|\nu|+|\mu|\geq 1} \frac{1}{\nu!\mu!} g_{\nu\mu} w^\nu \beta^\mu,$$

while the Taylor series of H and V are unknown

$$H(w, \beta) = \sum_{|\nu|+|\mu|\geq 1} \frac{1}{\nu!\mu!} h_{\nu\mu} w^\nu \beta^\mu, \qquad V(\beta) = \sum_{|\mu|\geq 1} \frac{1}{\mu!} v_\mu \beta^\mu.$$

Here ν and μ are multi-indices. Substituting these series in (5) and collecting coefficients of the $w^\nu\beta^\mu$-terms, we obtain linear systems, all of which must be solvable due to the existence of the center manifold. Fredholm's solvability condition for singular systems gives then expressions for $g_{\nu\mu}$ and v_μ in terms of the Taylor coefficients of $f(x, \alpha)$. For $\mu = 0$ this reproduces the critical normal form coefficients first computed in [16], while the coefficients with $|\mu| \geq 1$ yield the necessary data on the parameter dependence.

To summarize, a bifurcation point is detected within a certain small tolerance. As the prediction depends on the initial point, this translates into small errors of the predicted curve. If we start close enough to the actual new curve, any point will converge to it and in general one expects a convergence cone [14]. If we parametrize the predicted curve by ε, the initial amplitude ε is to be chosen within the convergence cone, see also Fig. 1.

This procedure is adopted from [3], where it has been applied to the derivation of the asymptotics of the fold and Hopf curves rooted at CP and BT codim 2 points, as well as that for a homoclinic orbit to a saddle emanating from the BT-point. Recently, this technique

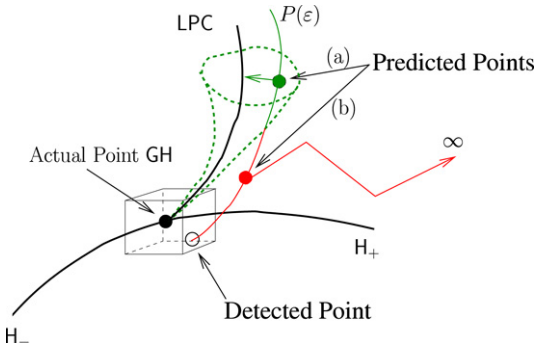

Fig. 1. Sketch of the switch in the case of a GH bifurcation. A predicted point along $P(\varepsilon)$ in the cone (a) will converge to the LPC-curve, outside (b) it will not.

has been successfully used for switching at codim 2 fixed points of maps to the continuation of nonhyperbolic periodic orbits rooted there [15]. Note that a similar procedure was suggested in [12], without using the Fredholm condition, and carried through in the ZH-case in [13], where, however, no asymptotics of codim 1 curves were derived. Finally, we point out that the problem of switching to the LPC-curve at the GH bifurcation has been briefly discussed in [3] in a setting without the Taylor expansion in β.

The paper is organized as follows. In Section 2 we recall smooth parameter-dependent normal forms on center manifolds for the GH, ZH and HH cases, and give the asymptotic expressions of the branches of nonhyperbolic cycles in these normal forms. Then we carry out the reduction procedure described above and derive the necessary coefficients $g_{\nu\mu}$, $h_{\nu\mu}$ and v_μ in terms of f and its derivatives. These coefficients are finally used to set up predictors for these branches in the original system (1). An implementation of the resulting formulas in the software MATCONT is discussed at the end of this section. Section 3 presents several applications of the technique developed in this paper to known ODE models, an extension of the Lorenz-84 system and a laser model, where we compare the asymptotic formulas for the cycle bifurcations with numerically computed LPC- and NS-branches. A discussion of existing results and open problems in switching to homoclinic branches at ZH and HH bifurcations is given in Section 4.

2. Asymptotics and the center manifold

2.1. The 'new' curves

The parameter-dependent normal forms are known and can be found in the standard texts, e.g. [17]. As the normal form and the asymptotic expressions are the necessary theoretical ingredient, we present these here.

2.1.1. Generalized Hopf

Near a GH bifurcation the vector field restricted to the center manifold is given by

$$\dot{w} = \lambda(\beta)w + c_1(\beta)w|w|^2 + c_2(\beta_2)w|w|^4 + \mathcal{O}(|w|^6), \quad w \in \mathbb{C}, \tag{6}$$

where $\lambda(0) = \mathrm{i}\omega$, and this bifurcation is characterized by $d_1 = \Re(c_1(0)) = 0$ and $d_2 = \Re(c_2(0)) \neq 0$. A curve LPC of fold bifurcation of limit cycles emanates from this point. Let us write $w = \rho e^{\mathrm{i}\psi}$, and, in particular,

$$\begin{aligned} &\lambda(\beta) = \mathrm{i}\omega + \beta_1 + \mathrm{i}b_1(\beta) + O(|\beta|^2), \\ &\Re(c_1(\beta)) = \beta_2 + O(|\beta|^2), \end{aligned} \tag{7}$$

where b_1 is a real function with $b_1(0) = 0$. To obtain the approximation to the LPC-curve, write (6) in polar coordinates

and truncate the sixth-order terms. Then the $\dot\rho$-equation decouples and a double equilibrium of this equation corresponds to the LPC-curve. The result is

$$\rho = \varepsilon, \qquad \beta_1 = d_2\varepsilon^4, \qquad \beta_2 = -2d_2\varepsilon^2. \tag{8}$$

2.1.2. Zero-Hopf

Near a ZH bifurcation the vector field restricted to the center manifold is given by

$$\begin{pmatrix}\dot x\\ \dot w\end{pmatrix} = \begin{pmatrix}\beta_1 + f_{200}x^2 + f_{011}|w|^2 + f_{300}x^3 + f_{111}x|w|^2\\ (\mathrm{i}\omega(\beta)+\beta_2)w + g_{110}xw + g_{210}x^2w + g_{021}w|w|^2\end{pmatrix} + \mathcal{O}(\|(x,w)\|^4), \tag{9}$$

where $(x, w) \in \mathbb{R}\times\mathbb{C}$. An extra Neimark–Sacker (torus) bifurcation of limit cycles (NS) occurs if $\Re(g_{110})f_{011} < 0$.

Using polar coordinates for w as for the GH-case and truncating fourth-order terms, the NS-curve is found as an equilibrium of the $(\dot x, \dot\rho)$-system together with the trace of the corresponding Jacobian, i.e. the Hopf condition for the amplitude system. The asymptotic expression is

$$\rho = \varepsilon, \qquad x = -\frac{f_{111}+2g_{021}}{2f_{200}}\varepsilon^2, \qquad \beta_1 = -f_{011}\varepsilon^2,$$
$$\beta_2 = \frac{2(\Re(g_{110}) - f_{200})\Re(g_{021}) + \Re(g_{110})f_{111}}{2f_{200}}\varepsilon^2. \tag{10}$$

This agrees with a formula given in [7].

2.1.3. Double-Hopf

For a HH bifurcation the dynamics on the center manifold is governed by the following normal form:

$$\begin{pmatrix}\dot w_1\\ \dot w_2\end{pmatrix} = \begin{pmatrix}(\mathrm{i}\omega_1(\beta)+\beta_1)w_1 + f_{2100}w_1|w_1|^2 + f_{1011}w_1|w_2|^2\\ (\mathrm{i}\omega_2(\beta)+\beta_2)w_2 + g_{1110}w_2|w_1|^2 + g_{0021}w_2|w_2|^2\end{pmatrix} + \mathcal{O}(\|(w_1,w_2)\|^4), \tag{11}$$

where $(w_1, w_2) \in \mathbb{C}\times\mathbb{C}$. There are generically two half-lines along which there is a NS bifurcation of limit cycles. Rewriting (11) in polar coordinates $w_1 = \rho_1 e^{\mathrm{i}\psi_1}$, $w_2 = \rho_2 e^{\mathrm{i}\psi_2}$, the two $\dot\rho$-equations decouple. With the fourth-order terms truncated, the asymptotics for the NS-curves are approximated by transcritical bifurcations of trivial equilibria of the reduced system (with either ρ_1 or ρ_2 equal to zero), which is equivalent to a vanishing determinant of the corresponding Jacobian. Their asymptotics are given as

$$(\rho_1, \rho_2, \beta_1, \beta_2) = \left(\varepsilon, 0, -\Re(f_{2100})\varepsilon^2, -\Re(g_{1110})\varepsilon^2\right), \tag{12}$$

$$(\rho_1, \rho_2, \beta_1, \beta_2) = \left(0, \varepsilon, -\Re(f_{1011})\varepsilon^2, -\Re(g_{0021})\varepsilon^2\right). \tag{13}$$

2.2. Coefficients of parameter-dependent center manifolds

We can assume that the codim 2 point is $x_0 = 0$ and $\alpha_0 = 0$. The homological equation (5) results in a formal power series, the coefficients of which should be zero, leading to a recursive procedure. This also requires the Taylor expansion of the right-hand side of (1)

$$f(x,\alpha) = Ax + \frac{1}{2}B(x,x) + \frac{1}{6}C(x,x,x) + \frac{1}{24}D(x,x,x,x) + J_1\alpha + A_1(x,\alpha) + \frac{1}{2}B_1(x,x,\alpha) + \frac{1}{6}C_1(x,x,x,\alpha) + \cdots, \tag{14}$$

where A is the Jacobian of f w.r.t. to x and we have defined

$$B(u,v) = \sum_{i,j=1}^{n}\frac{\partial^2 f(x_0,\alpha_0)}{\partial x_i\partial x_j}u_iv_j,$$

$$C(u,v,w) = \sum_{i,j,k=1}^{n}\frac{\partial^3 f(x_0,\alpha_0)}{\partial x_i\partial x_j\partial x_k}u_iv_jw_k,$$

$$J_1u = \sum_{i=1}^{2}\frac{\partial f(x_0,\alpha_0)}{\partial\alpha_i}u_i,$$

$$A_1(u,v) = \sum_{i=1}^{n}\sum_{j=1}^{2}\frac{\partial^2 f(x_0,\alpha_0)}{\partial x_i\partial\alpha_j}u_iv_j,$$

and similarly D, B_1 and C_1.

We assume that the critical normal form coefficients are known (see [16,3]) and give here only parameter-related coefficients $h_{\nu\mu}$ from the homological equation. These provide in each case a linear approximation to the parameter transformation (3).

2.2.1. Generalized Hopf

Here we closely follow the idea outlined in [3]. We first expand the eigenvalue and the first Lyapunov coefficient in the original parameters α

$$\lambda(\alpha) = \mathrm{i}\omega + \gamma_{1,10}\alpha_1 + \gamma_{1,01}\alpha_2 + \cdots,$$
$$c_1(\alpha) = \Im(c_1(0)) + \gamma_{2,10}\alpha_1 + \gamma_{2,01}\alpha_2 + \cdots,$$

i.e. we assume $\alpha = \beta$ and insert this into the normal form (6). We then collect the equations to obtain the transformation to the unfolding parameters β. Below we have $\mu = (10), (01)$ as indices and $v_{10} = (1, 0)$, $v_{01} = (0, 1)$ as vectors.

The first equation in the homological equation comes from the coefficient of the w-term, i.e. $\nu = (10)$ and $\mu = (00)$, and gives the (eigenvalue) equation

$$(A - \mathrm{i}\omega I_n)h_{1000} = 0.$$

In what follows we write $q = h_{1000}$. The $\nu = (01)$ and $\mu = (00)$ coefficient is the complex conjugated version and will be omitted as it does not provide new information. To impose the Fredholm solvability condition we need the adjoint eigenvector p defined by $(A + \mathrm{i}\omega I_n)^T p = 0$. We also normalize so that $\bar q^T q = \bar p^T q = 1$.

The formula for the Lyapunov coefficient c_1 on the center manifold is derived from the terms in (5) with $\mu = (00)$ and $\nu = (20), (11), (21)$, see [17]. These are

$$(A - 2\mathrm{i}\omega I_n)h_{2000} = -B(q,q), \tag{15a}$$

$$Ah_{1100} = -B(q,\bar q), \tag{15b}$$

$$(A - \mathrm{i}\omega I_n)h_{2100} = 2c_1q - (C(q,q,\bar q) + 2B(h_{1100},q) + B(h_{2000},\bar q)). \tag{15c}$$

Now (15a) and (15b) are non-singular and one can easily obtain h_{2000} and h_{1100}. The matrix in (15c) is singular so that imposing Fredholm's solvability condition leads to the following compact formula for the first Lyapunov coefficient

$$c_1 = \frac{1}{2}\bar p^T\left(C(q,q,\bar q) + 2B(h_{1100},q) + B(h_{2000},\bar q)\right). \tag{16}$$

Considering $\nu = (00)$ and $\nu = (10)$, i.e. the β_1, β_2, $\beta_1 w$ and $\beta_2 w$ terms, the first parameter-dependent equations (actually four) coming from (5) are

$$\begin{aligned} Ah_{00\mu} &= -J_1v_\mu,\\ (A - \mathrm{i}\omega I_n)h_{10\mu} &= \gamma_{1,\mu}q - A_1(q,v_\mu) - B(q,h_{00\mu}).\end{aligned} \tag{17}$$

The first equation is non-singular, so we set $h_{00\mu} = A^{-1}J_1v_\mu$. From the second we find the two $\gamma_{1,\mu}$ using the Fredholm alternative

$$\gamma_{1,\mu} = \bar p^T\left(A_1(q,v_\mu) - B(q,A^{-1}J_1v_\mu)\right). \tag{18}$$

The vectors $h_{10\mu}$ will be needed and can be obtained using a bordered matrix approach, see [10],

$$\begin{pmatrix} A - \mathrm{i}\omega I_n & q \\ \bar{p}^T & 0 \end{pmatrix} \begin{pmatrix} h_{10\mu} \\ 0 \end{pmatrix} = \begin{pmatrix} \gamma_{1,\mu} q - A_1(q, v_\mu) - B(q, h_{00\mu}) \\ 0 \end{pmatrix}. \tag{19}$$

The vector h_{2100} can also be obtained in this way. This choice for the bordering vectors leads to solutions such that $\bar{p}^T h_{10\mu} = \bar{p}^T h_{2100} = 0$.

The higher-order parameter-dependent equations from (5) originate from the terms with $\mu = (10), (01)$ and $\nu = (20), (11), (21)$:

$$\begin{aligned}(A - 2\mathrm{i}\omega I_n) h_{20\mu} &= 2h_{2000}\gamma_{1,\mu} - \big[C(q, q, h_{00\mu}) + 2B(q, h_{10\mu}) \\ &\quad + B(h_{2000}, h_{00\mu}) + B_1(q, q, v_\mu) + A_1(h_{2000}, v_\mu)\big], \qquad (20a)\\ A h_{11\mu} &= 2\Re(\gamma_{1,\mu}) h_{1100} - \big[C(q, \bar{q}, h_{00\mu}) + B(h_{1100}, h_{00\mu}) \\ &\quad + B(\bar{q}, h_{10\mu}) + B(q, h_{01\mu}) + B_1(q, \bar{q}, v_\mu) + A_1(h_{1100}, v_\mu)\big], \qquad (20b)\\ (A - \mathrm{i}\omega I_n) h_{21\mu} &= 2\gamma_{2,\mu} q + h_{2100}(2\gamma_{1,\mu} + \bar{\gamma}_{1,\mu}) + 2h_{10\mu} c_1 \\ &\quad - \big[D(q, q, \bar{q}, h_{00\mu}) + 2C(q, h_{1100}, h_{00\mu}) + 2C(q, \bar{q}, h_{10\mu}) \\ &\quad + C(q, q, h_{01\mu}) + C(h_{2000}, \bar{q}, h_{00\mu}) + 2B(q, h_{11\mu}) \\ &\quad + 2B(h_{1100}, h_{10\mu}) + B(h_{2000}, h_{01\mu}) + B(h_{2100}, h_{00\mu}) \\ &\quad + B(h_{20\mu}, \bar{q}) + C_1(q, q, \bar{q}, v_\mu) + 2B_1(h_{1100}, q, v_\mu) \\ &\quad + B_1(h_{2000}, \bar{q}, v_\mu) + A_1(h_{2100}, v_\mu)\big]. \qquad (20c)\end{aligned}$$

Now, as before, (20a) and (20b) are non-singular so we can solve these to get $h_{20\mu}$ and $h_{11\mu}$. With the Fredholm alternative we find

$$\begin{aligned}\gamma_{2,\mu} &= \frac{1}{2}\bar{p}^T \big[D(q, q, \bar{q}, h_{00\mu}) + 2C(q, h_{1100}, h_{00\mu}) \\ &\quad + 2C(q, \bar{q}, h_{10\mu}) + C(q, q, h_{01\mu}) + C(h_{2000}, \bar{q}, h_{00\mu}) \\ &\quad + 2B(q, h_{11\mu}) + 2B(h_{1100}, h_{10\mu}) + B(h_{2000}, h_{01\mu}) \\ &\quad + B(h_{2100}, h_{00\mu}) + B(h_{20\mu}, \bar{q}) + C_1(q, q, \bar{q}, v_\mu) \\ &\quad + 2B_1(h_{1100}, q, v_\mu) + B_1(h_{2000}, \bar{q}, v_\mu) + A_1(h_{2100}, v_\mu)\big]. \qquad (21)\end{aligned}$$

The parameter transformation (3) to get to the form (7) is given by

$$\alpha = \left(\Re \begin{pmatrix} \gamma_{1,10} & \gamma_{1,01} \\ \gamma_{2,10} & \gamma_{2,01} \end{pmatrix}\right)^{-1} \beta. \tag{22}$$

A careful inspection shows that every term in (21) is obtained by differentiating the corresponding one in (16) to a parameter. So essentially, we get a Taylor expansion of the Lyapunov coefficient. As an alternative computational scheme, one can normalize immediately in (17). This results in an orthogonal frame for the parameter transformation, i.e. along the Hopf curve and perpendicularly. Then the higher-order equations (20) should be considered for these orthogonal vectors to obtain linear scalings for the correct parameter transformation. We will use this scheme for the next case.

2.2.2. Zero-Hopf

This case is also treated in [13], however with only one parameter and for hyperbolic periodic orbits. Thus our computational scheme is different. We introduce the eigenvectors

$$A q_1 = A^T p_1 = 0 \quad \text{and} \quad A q_2 = \mathrm{i}\omega q_2, \qquad A^T p_2 = -\mathrm{i}\omega p_2,$$

normalized so that $\bar{q}_i^T q_i = \bar{p}_i^T q_i = 1$ for $i = 1, 2$. We list only the necessary equations:

$$A[h_{00010},\ h_{00001}] = [q_1,\ 0] - J_1[v_{10},\ v_{01}], \tag{23a}$$

$$\begin{aligned}A[h_{10010},\ h_{10001}] &= [h_{20000},\ 0] - A_1(q_1, [v_{10}, v_{01}]) \\ &\quad - B(q_1, [h_{00010},\ h_{00001}]), \qquad (23b)\\ (A - \mathrm{i}\omega I_n)[h_{01010},\ h_{01001}] &= [h_{11000},\ q_2] - A_1(q_2, [v_{10},\ v_{01}]) \\ &\quad - B(q_2, [h_{00010},\ h_{00001}]). \qquad (23c)\end{aligned}$$

In contrast to the other cases, GH and HH, here the first system is already singular. Taking the inner-product with the adjoint null-vector we obtain the new orthogonal frame (s_1, s_2)

$$\begin{aligned}\gamma = (\gamma_1, \gamma_2) = p_1^T J_1, \qquad s_1^T = \gamma / \|\gamma\|^2, \qquad s_2^T = (-\gamma_2, \gamma_1), \\ v_{10} = s_1 + \delta_1 s_2, \qquad v_{01} = \delta_2 s_2.\end{aligned} \tag{24}$$

Polynomial terms in the normal form (9) like $\beta_1 x$ are also resonant, but they can be eliminated by hypernormalization. After solving (23a) with a bordered matrix, still a multiple of q_1 may be added to h_{00010} and h_{00001}. We use this to perform hypernormalization. If we write

$$r_1 = -A^{INV} \begin{pmatrix} q_1 - J_1 s_1 \\ 0 \end{pmatrix}, \qquad r_2 = -A^{INV} \begin{pmatrix} -J_1 s_2 \\ 0 \end{pmatrix},$$

where A^{INV} indicates the use of a bordered matrix (using the vectors q_1 and p_1), then we have

$$h_{00010} = r_1 + \delta_1 r_2 + \delta_3 q_1, \qquad h_{00001} = \delta_2 r_2 + \delta_4 q_1,$$

for some δ's. Then by applying the Fredholm alternative to (23b) and (23c) we can solve for all δ's at once

$$\begin{aligned} LL \begin{pmatrix} \delta_1 \\ \delta_3 \end{pmatrix} &= -\begin{pmatrix} \langle p_1, A_1(q_1, r_1) + B(q_1, r_1)\rangle \\ \langle p_2, A_1(q_2, r_1) + B(q_2, r_1)\rangle \end{pmatrix}, \\ \Re(LL) \begin{pmatrix} \delta_2 \\ \delta_4 \end{pmatrix} &= \begin{pmatrix} 0 \\ 1 \end{pmatrix}, \end{aligned} \tag{25}$$

where

$$LL = \begin{pmatrix} \langle p_1, A_1(q_1, r_2) + B(q_1, r_2)\rangle & 2f_{200} \\ \langle p_2, A_1(q_2, r_2) + B(q_2, r_2)\rangle & g_{110} \end{pmatrix}.$$

In particular, this also defines the parameter transformation (3).

2.2.3. Double Hopf

Although high-dimensional, this case can be treated in a relatively simple manner. We introduce the eigenvectors

$$A q_i = \mathrm{i}\omega q_i, \qquad A^T p_i = -\mathrm{i}\omega p_i,$$

normalized so that $\bar{q}_i^T q_i = \bar{p}_i^T q_i = 1$ for $i = 1, 2$.

Using the same notation as for the generalized Hopf from (5) we get

$$\begin{aligned} A h_{0000\mu} &= -J_1 v_\mu, \\ (A - \mathrm{i}\omega_1 I_n) h_{1000\mu} &= \gamma_{1,\mu} q_1 - A_1(q_1, v_\mu) - B(q_1, h_{0000\mu}), \\ (A - \mathrm{i}\omega_2 I_n) h_{0010\mu} &= \gamma_{2,\mu} q_2 - A_1(q_2, v_\mu) - B(q_2, h_{0000\mu}). \end{aligned} \tag{26}$$

As the first equation is non-singular, formal substitution of h_{000010} and h_{000001} and the Fredholm alternative leads to the same transformation (22) from the unfolding to the system parameters.

2.3. Implementation of the predictors

We have implemented our switching routines in MATCONT [6]. For the continuation of LPC and NS curves it uses a minimally augmented defining system [18], i.e. we need to supply an approximation of the limit cycle, the period, the parameters and, if necessary, the multiplier. The parameters follow from applying the inverse transformation to (3). There is always one dynamic variable ψ giving a free phase shift along the bifurcating limit cycle with a period $\frac{2\pi}{\omega_1(\varepsilon)}$. For the initial cycle we make an equidistant mesh $\psi = 2n\pi/mN$, $n = 0 \ldots mN$ where $N + 1$ is the number of mesh points and m the number of collocation points. Let q denote the eigenvector corresponding to the eigenvalue $\mathrm{i}\omega_1$, then points on the limit cycle are given by $x_0 + \varepsilon(q\mathrm{e}^{\mathrm{i}\psi} + \bar{q}\mathrm{e}^{-\mathrm{i}\psi})$. Similarly, terms as $\varepsilon^2 h_{20}\mathrm{e}^{2\mathrm{i}\psi}$ and $\varepsilon^2 h_{0010}$ are included. An internal routine of MATCONT then adapts this limit cycle on each mesh interval

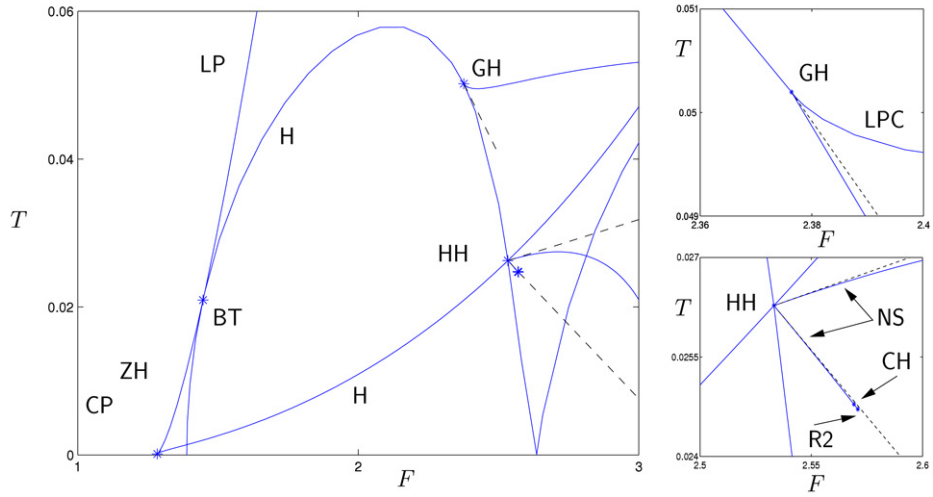

Fig. 2. Bifurcation diagram of the Extended Lorenz-84 model. Labels are as in the text except LP Limit Point and H Hopf. Dashed lines show the predicted new curves; (a) Zoom near the GH point, (b) Zoom near the HH point. On the lower NS curve two codim 2 bifurcations of cycles are detected: CH Chenciner bifurcation, R2 1:2 Resonance.

from an equidistant mesh to a mesh defined at the non-equidistant collocation points.

For the NS curves the system is augmented with the real part k of the multiplier. In this case the normal forms (9), (11) also define a second rotation with frequency $\omega_2(\varepsilon)$ and we have the multiplier $k = \cos\left(\frac{2\pi\omega_2(\varepsilon)}{\omega_1(\varepsilon)}\right)$.

MATCONT uses Moore–Penrose continuation for which also a tangent vector to the bifurcation curve is needed. This tangent vector is easily obtained by differentiating the predictor w.r.t. ε.

Below we list some case-specific details.

2.3.1. Generalized Hopf

The period is given by $T = 2\pi/\omega + (2d_2b_{1,2} - \Im(c_1(0)))\varepsilon^2$, with $b_{1,2} = \frac{\partial b_1}{\partial \beta_2}$. The parameters are given by $\alpha = \alpha_0 + V(0, -2d_2\varepsilon^2)^T$. The cycle is approximated by

$$x_0 + \varepsilon(qe^{i\psi} + \bar{q}e^{-i\psi}) + \varepsilon^2(h_{2000}e^{2i\psi} + h_{0200}e^{-2i\psi} + h_{1100} - 2d_2(h_{0010}V_{12} + h_{0001}V_{22})).$$

Note that for a ε^4-approximation also seventh-order derivatives would be needed; this follows from Remark 3.3.2 in [21]. Therefore we restrict to $\mathcal{O}(\varepsilon^3)$ in the implementation.

2.3.2. Zero-Hopf

The cycle is approximated by

$$x_0 + \varepsilon(q_2e^{i\psi} + \bar{q}_2e^{-i\psi}) + \varepsilon^2(h_{02000}e^{2i\psi} + h_{00200}e^{-2i\psi} + h_{01100}) + \beta_1h_{00010} + \beta_2h_{00010} + xq_1,$$

where x, β_1, β_2 are as in (10). In the continuation we also need to provide the period and the multiplier. Approximating formulas are defined as follows

$$T = 2\pi/\omega(0) - \varepsilon^2(\omega_1\beta_1 + \omega_2\beta_2 + \Im(g_{110})x - \Im(g_{021})), \quad k = 1 - (4\pi\Re(g_{110})f_{011})(\varepsilon/\omega_0)^2. \tag{27}$$

2.3.3. Double Hopf

On the first branch the cycle is approximated by

$$x_0 + \varepsilon(q_1e^{i\psi} + \bar{q}_1e^{-i\psi}) + \varepsilon^2(h_{200000}e^{2i\psi} + h_{020000}e^{-2i\psi} + h_{110000} + A^{-1}J_1V\Re(f_{2100}, g_{1110})^T).$$

Approximating formulas for the period and the multiplier on the first branch are given by

$$T = \frac{2\pi}{\omega_1 + d\omega_1\varepsilon^2}, \qquad k = \cos(T(\omega_2 + d\omega_2\varepsilon^2)), \quad (d\omega_1, d\omega_2) = -\Im(\gamma_1\gamma_2)^T(\Re(\gamma_1\gamma_2)^T)^{-1} \times \Re(f_{2100}, g_{1110})^T + \Im(f_{2100}, g_{1110}) \tag{28}$$

and similarly for the other branch.

3. Examples

3.1. New curves in an extension of the Lorenz-84 model

The first example is an extended version of the Lorenz-84 model. A bifurcation analysis of this model was presented in [22,23]. In this system X models the intensity of a baroclinic wave and Y and Z the sine and cosine coefficients of the wave. This model may be extended with a variable U to study the influence of external parameters such as temperature, and the model then shows several limit cycle bifurcations [20]. It has the form:

$$\begin{cases} \dot{X} = -Y^2 - Z^2 - \alpha X + \alpha F - \gamma U^2, \\ \dot{Y} = XY - \beta XZ - Y + G, \\ \dot{Z} = \beta XY + XZ - Z, \\ \dot{U} = -\delta U + \gamma UX + T. \end{cases} \tag{29}$$

The parameters F and T are varied while we fix $\alpha = .25$, $\beta = 1$, $G = .25$, $\delta = 1.04$, $\gamma = .987$. The bifurcation diagram displays one fold bifurcation and two Hopf bifurcation curves, see Fig. 2. We find all codim 2 points of equilibria, in particular, GH, ZH and HH, see Table 1.

We have applied our switching routines to all three emanating curves, since the NS bifurcation from ZH is a neutral saddle. The predictions in parameter space are shown in Fig. 2 next to the numerically continued curves. The predicted points were used as a starting point for the continuation of these limit cycle bifurcations, which shows that our approach works. Another numerical check is provided by inspecting the tangent vector, which we provide together with a first point. When we find a second point on the curve by continuation and adapt the defining system, we will obtain a more precise tangent vector. For a small continuation step, this tangent vector and the predicted one should be close. Indeed, for the examples reported here, the first digits always coincided.

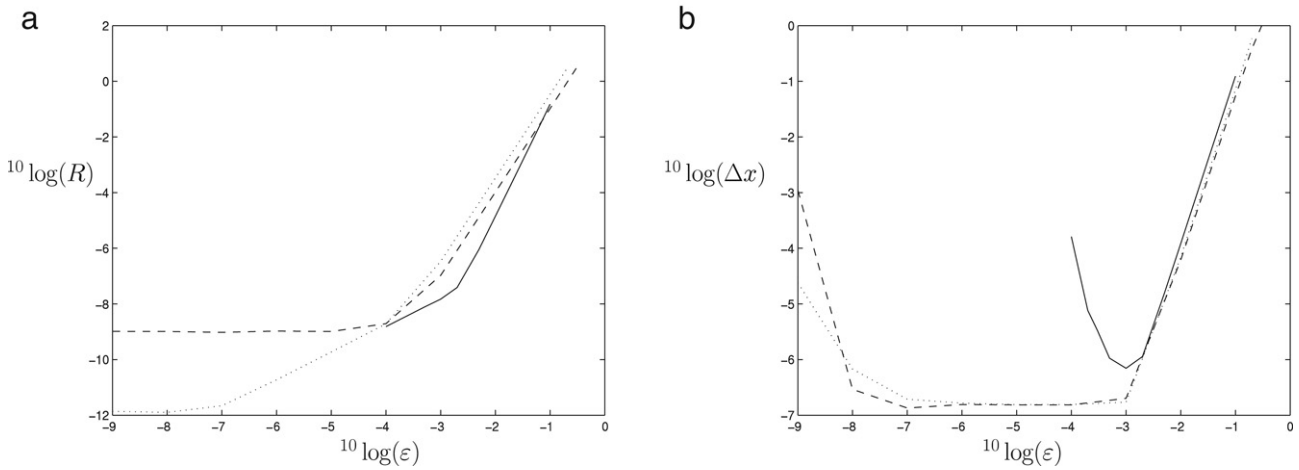

Fig. 3. Error measures: (a) The residual R of the first Newton-step. (b) The distance d between the predicted and the first corrected point. In this computation, we left out the tangent vector in the continuation. MATCONT then tries to correct the first point immediately instead of starting the continuation. We have taken 20 mesh and 4 collocation points and $\varepsilon \in [10^{-9}, .2]$. The points shown correspond to a choice for ε where the predicted point converged to the codim 1 curve. Lines correspond to bifurcation curves in Fig. 2 as follows: LPC solid, lower NS dashed, upper NS dotted.

Table 1
Parameter values of F and T at the bifurcation points in Fig. 2 together with normal coefficients (scaled, see [17])

Label	F	T	Normal form coefficients
GH	2.3763601	.050197432	$d_2 = 0.1558012$
HH	2.5332211	.026273943	$p_{11}p_{22} = -1, \theta = -3.648550, \delta = -1.052987$ $\Theta = 1230.630, \Delta = -210.861$
ZH	1.2834193	.000126541	$s = 1, \theta = 0.3715145, E = -1$

Finally we present some measure of the error of the switching routines as a function of the initial amplitude ε, see Fig. 3 and its caption. Interestingly, this figure represents the idea of Fig. 1. Using a small initial amplitude ε may not work due to a numerical error in the calculated codim 2 point. On the other hand ε must not be taken too large for the approximation to remain valid.

3.2. Switching in a Laser model

In [24] a single-mode inversionless laser with a three-level phaser was studied and shown to operate in various modes. These modes are "off" (non-lasing), continuous waves, periodic, quasi-periodic and chaotic lasing. In particular, the boundary of the region of chaos seems to be defined by several limit cycle bifurcations born from several codim 2 equilibrium bifurcations. Here we start such boundary computations using our routines without first doing simulations and limit cycle continuations in this 9-dimensional system.

The model is a 9-dimensional system given by 3 real and 3 complex equations:

$$\begin{cases} \dot{\Omega}_l = -\dfrac{\gamma_{cav}}{2}\Omega_l - g\Im(\sigma_{ab}), \\ \dot{\rho}_{aa} = R_a - \dfrac{\mathrm{i}}{2}(\Omega_l(\sigma_{ab} - \sigma_{ab}^*) + \Omega_p(\sigma_{ac} - \sigma_{ac}^*)), \\ \dot{\rho}_{bb} = R_b + \dfrac{\mathrm{i}}{2}\Omega_l(\sigma_{ab} - \sigma_{ab}^*), \\ \dot{\sigma}_{ab} = -(\gamma_1 + \mathrm{i}\Delta_l)\sigma_{ab} - \dfrac{\mathrm{i}}{2}(\Omega_l(\rho_{aa} - \rho_{bb}) - \Omega_p\sigma_{cb}), \\ \dot{\sigma}_{ac} = -(\gamma_2 + \mathrm{i}\Delta_p)\sigma_{ac} - \dfrac{\mathrm{i}}{2}(\Omega_p(2\rho_{aa} + \rho_{bb} - 1) - \Omega_l\sigma_{cb}^*), \\ \dot{\sigma}_{cb} = -(\gamma_3 + \mathrm{i}(\Delta_l - \Delta_p))\sigma_{cb} - \dfrac{\mathrm{i}}{2}(\Omega_l\sigma_{ac}^* - \Omega_p\sigma_{ab}), \end{cases} \tag{30}$$

with $R_a = -.505\rho_{aa} - .405\rho_{bb} + .45$, $R_b = .0495\rho_{aa} - .0505\rho_{bb} + .0055$ and $\Delta_l := \Delta_{cav} + g\Re(\sigma_{ab})/\Omega_l$. The parameters are fixed at

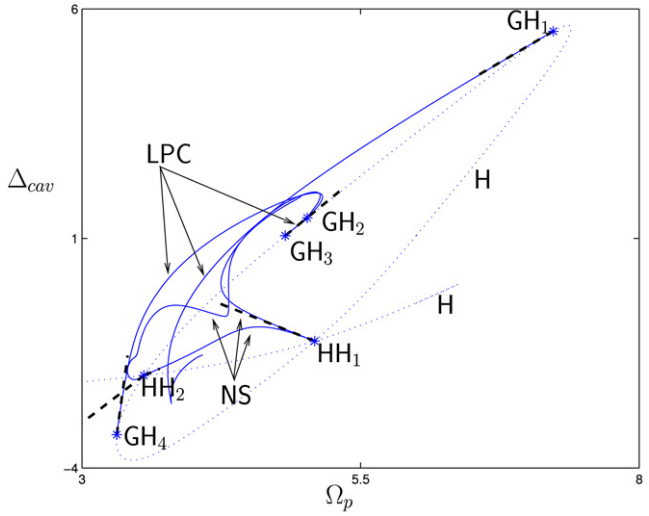

Fig. 4. Partial bifurcation diagram of the inversionless laser. Hopf curves (denoted by H) are dotted, while LPC and NS curves are solid. Dashed lines show the predicted approximations to the new curves.

$\gamma_1 = .05$, $\gamma_2 = .25525$, $\gamma_3 = .25025$, $\gamma_{cav} = .03$, $g = 100$, $\Delta_p = 0$ while Δ_{cav} and Ω_p are varied to study several detuning effects. For more details, see [24].

We have reproduced a part from the bifurcation diagram which corresponds to continuous wave and periodically pulsating solutions, i.e. with $\Omega_l \neq 0$, see Fig. 4. As the system has $\mathbb{Z}_2$-symmetry the same bifurcations are found for $\Delta_{cav} \to -\Delta_{cav}$. For clarity of the figure we do not display these here. We list the codim 2 points in Table 2. The normal form coefficients of HH$_1$ confirm the claim of [24] that the most complicated type was encountered; only the 3-torus is stable. This is also confirmed when we continue the Neimark–Sacker bifurcations. For HH$_2$ the NS curves are not in the same quadrant defined by the Hopf curves, while they are for

Table 2
Parameter values of Ω_p and Δ_{cav} at the codim 2 points together with normal coefficients (scaled, see [17])

Label	Ω_p	Δ_{cav}	Normal form coefficients
GH_1	7.228819	5.511455	$d_2 = -46.49852$
GH_2	5.021574	1.446387	$d_2 = 3.813132$
GH_3	4.824066	1.059367	$d_2 = 195.1119$
GH_4	3.312120	−3.273568	$d_2 = -6.468468$
HH_1	5.087299	−1.2362053	$p_{11}p_{22} = -1, \theta = -.07194543, \delta = -13.91412$ $\Theta = .9595389, \Delta = -2602.275$
HH_2	3.555848	−1.983857	$p_{11}p_{22} = 1, \theta = -.1179924, \delta = -26.59452$ $\Theta = -10.81042, \Delta = -2713.608$

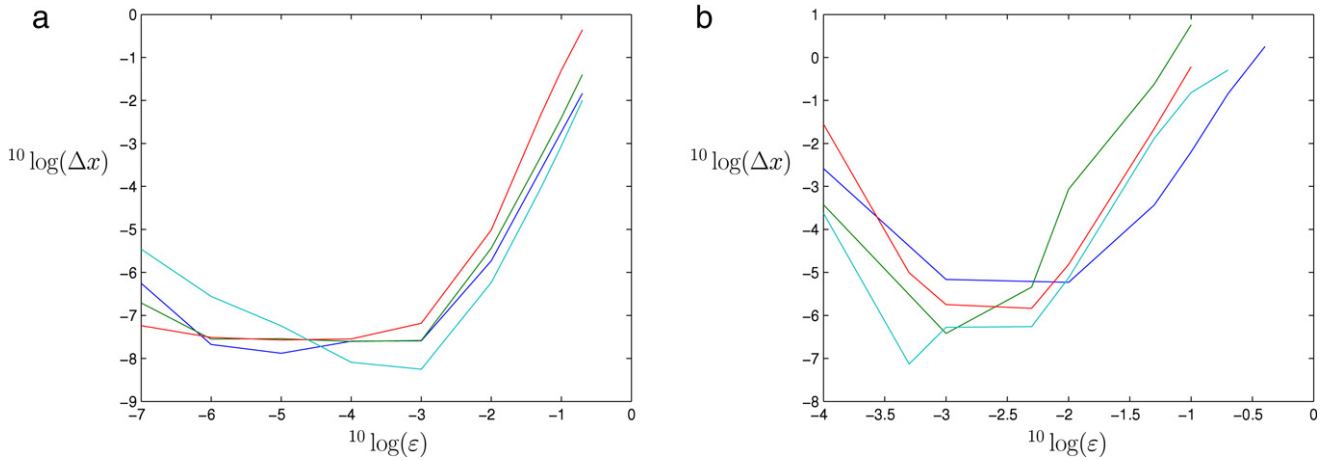

Fig. 5. Error measures along the eight curves: ^{10} log of the distance between the predicted and the first corrected point versus $^{10}\log(\varepsilon)$. (a) Along the Neimark–Sacker curves, (b) Along the LPC curves. This figure again resembles the idea of Fig. 1.

HH_1. All cycle bifurcations where computed with 20 mesh points and 4 collocation points and the initial amplitude was set to $\varepsilon = .001$, which worked immediately in all cases. The error measures are shown in Fig. 5 showing similar behaviour as Fig. 3(b). We remark that one LPC curve connects GH_2 and GH_3 points and stays close to the Hopf curve. Similarly, a NS curve starts at HH_1, becomes neutral between two 1:2 resonances and ends at HH_2. It would have taken much more effort to find this feature otherwise.

4. Discussion

This paper contributes to the bifurcation analysis of codim 2 bifurcations of equilibria in multidimensional ODEs by providing explicit predictors for branches of nonhyperbolic cycles emanating from these bifurcations. We have tested it on several examples with good results. We believe that this work will further facilitate automated analysis of nonlinear systems. However, we like to mention that we also tried the double Hopf point in a model for the lateral pyloric neuron [8,9]. Although we were able to switch to one branch and continue it without any problem, the Jacobian of the defining system along the second branch was numerically singular. In this model with multiple time scales probably a special numerical scheme is necessary.

It is well known that branches of orbits homoclinic to hyperbolic equilibria are also rooted at BT, ZH and HH codim 2 bifurcation points. The BT case has been treated in [2] (see also [3], where the computational setting is closest to the present paper). The corresponding predictor for the homoclinic branch is implemented in MATCONT. The problem of providing predictors for homoclinic branches rooted at ZH and HH points is more challenging. Some important results in this direction are obtained in [4,7,5], where the systems reduced to the center manifold were considered. However, a complete set of formulas suitable for switching to homoclinic curves in these cases is still not available. For instance, in the ZH case the normal form (9) exhibits homoclinic bifurcations of saddle-focus equilibria in the parameter plane along a bifurcation curve with the linear approximation

$$\beta_{2,hom} = \frac{\Re(g_{110})\beta_1}{f_{200}(2f_{200} - 3\Re(g_{110}))}\left[\Re(g_{210}) - \frac{3\Re(g_{110})}{2f_{200}}f_{300} + \frac{(f_{200} - \Re(g_{110}))}{f_{011}}f_{111} - \frac{2(f_{200} - \Re(g_{110}))^2}{f_{011}\Re(g_{110})}\Re(g_{021})\right],$$

provided that $\Re(g_{110})f_{011} < 0$ and $\Re(g_{110})f_{200} < 0$. Application of the above reduction to the parameter-dependent center manifolds in the ZH case yields an approximation to the bifurcation curve in the parameter plane. Now the challenge is to construct a suitable initial solution in state space. On this work in progress will be reported elsewhere.

Another direction for future research is a problem of switching to secondary cycle bifurcations at codim 2 bifurcations of cycles in (1). Here a generalization of the periodic normalization technique from [18] to critical codim 2 cases and its extension to parameter-dependent systems in the spirit of [15] are required.

Acknowledgement

The authors want to thank S. Wieczorek for suggesting the laser model and his further assistance with it.

References

[1] V.I. Arnold, Geometrical Methods in the Theory of Ordinary Differential Equations, Springer-Verlag, New York, Heidelberg, Berlin, 1983.
[2] W.-J. Beyn, Numerical analysis of homoclinic orbits emanating from a Takens-Bogdanov point, IMA J. Numer. Anal. 14 (1994) 381–410.
[3] W.-J. Beyn, A. Champneys, E. Doedel, W. Govaerts, Yu.A. Kuznetsov, B. Sandstede, Numerical continuation, and computation of normal forms, in: B. Fiedler (Ed.), Handbook of Dynamical Systems, vol. 2, Elsevier Science, Amsterdam, 2002, pp. 149–219.

[4] H.W. Broer, G. Vegter, Subordinate Šil'nikov bifurcations near some singularities of vector fields having low codimension, Ergodic Theory Dynam. Systems 4 (1984) 509–525.
[5] A.R. Champneys, V. Kirk, The entwined wiggling of homoclinic curves emerging from saddle-node/Hopf instabilities, Physica D 195 (2004) 77–105.
[6] A. Dhooge, W. Govaerts, Yu.A. Kuznetsov, MATCONT:A MATLAB package for numerical bifurcation analysis of ODEs, ACM Trans. Math. Software 29 (2003) 141–164.
[7] P. Gaspard, Local birth of homoclinic chaos, Physica D 62 (1993) 94–122.
[8] W. Govaerts, J. Guckenheimer, A. Khibnik, Defining functions for multiple Hopf bifurcations, SIAM J. Numer. Anal. 34 (3) (1997) 1269–1288.
[9] W. Govaerts, Yu.A. Kuznetsov, B. Sijnave, Numerical methods for the generalized Hopf bifurcation, SIAM J. Numer. Anal. 38 (1) (2000) 329–346.
[10] W.J.F Govaerts, Numerical Methods for Bifurcations of Dynamical Equilibria, SIAM, Philadelphia, 2000.
[11] J. Guckenheimer, P. Holmes, Nonlinear Oscillations, Dynamical Systems and Bifurcations of Vector Fields, Springer-Verlag, New York, 1983.
[12] M. Ipsen, F. Hynne, P.G. Sørensen, Systematic derivation of amplitude equations and normal forms for dynamical systems, Chaos 8 (1998) 834–852.
[13] M. Ipsen, F. Hynne, P.G Sørensen, Amplitude equations for reaction-diffusion systems with a Hopf bifurcation and slow real modes, Physica D 136 (2000) 66–92.
[14] A.D Jepson, D.W Decker, Convergence cones near bifurcation, SIAM J. Numer. Anal. 23 (1986) 959–975.
[15] R. Khoshsiar Ghaziani, W. Govaerts, Yu.A. Kuznetsov, H.G.E Meijer, Numerical methods for two-parameter local bifurcation analysis of maps, SIAM J. Sci. Comput. 29 (2007) 2644–2667.
[16] Yu.A. Kuznetsov, Numerical normalization techniques for all codim 2 bifurcations of equilibria in ODEs, SIAM J. Numer. Anal. 36 (1999) 1104–1124.
[17] Yu.A. Kuznetsov, Elements of Applied Bifurcation Theory, third edition, Springer-Verlag, New York, 2004.
[18] Yu.A. Kuznetsov, W. Govaerts, E.J Doedel, A. Dhooge, Numerical periodic normalization for codim 1 bifurcations of limit cycles, SIAM J. Numer. Anal. 43 (2005) 1407–1435.
[19] Yu.A. Kuznetsov, V.V Levitin, CONTENT: A multiplatform environment for analyzing dynamical systems. ftp.cwi.nl/pub/CONTENT. 1995–1997.
[20] Yu.A. Kuznetsov, H.G.E Meijer, L. van Veen, The fold-flip bifurcation, Internat. J. Bifur. Chaos 14 (2004) 2253–2282.
[21] H.G.E Meijer, Codimension 2 bifurcations of iterated maps. Ph.D. Thesis, Utrecht University, Netherlands, 2006.
[22] A. Shil'nikov, G. Nicolis, C. Nicolis, Bifurcation and predictability analysis of a low-order atmospheric circulation model, Internat. J. Bifur. Chaos 5 (1995) 1701–1711.
[23] L. van Veen, Baroclinic flow and the Lorenz-84 model, Internat. J. Bifur. Chaos 13 (2003) 2117–2139.
[24] S. Wieczorek, W.W Chow, Self-induced chaos in a single-mode inversionless laser, Phys. Rev. Lett. 97 (2006) 113903.